Activity-composition relations in the system $CaCO_3$ - $MgCO_3$ predicted from static structure energy calculations and Monte Carlo simulations

Victor L. Vinograd[1], Benjamin P. Burton[2], Julian D. Gale[3], Neil L. Allan[4]

and Björn Winkler[1]

[1]Institut für Geowissenschaften, Universität Frankfurt, Frankfurt a.M., Germany
[2]Ceramics Division, National Institute of Standards, Gaithersburg, USA
[3]Nanochemistry Research Institute, Curtin University, Perth, WA
[4]School of Chemistry, University of Bristol, Bristol, UK

28th June 2006

Abstract

Thermodynamic mixing properties and subsolidus phase relations of the rhombohedral carbonate system, (1-x)·$CaCO_3$-x·$MgCO_3$, were modelled with static structure energy calculations based on well constrained empirical interatomic potentials. Relaxed static structure energies of a large set of randomly selected structures in a 4x4x1 supercell of $R\bar{3}c$ calcite (a = 4.988 Å, c = 17.061Å) were calculated with the General Utitility Lattice Program (GULP). These energies were cluster expanded in a basis set of 12 pair-wise effective interactions. Temperature-dependent enthalpies of mixing were calculated by the Monte Carlo method. Free energies of mixing were obtained by thermodynamic integration of the Monte Carlo results. The calculated phase diagram is in good agreement with experimental phase boundaries.

Keywords: A. Monte Carlo simulations; B. Rhombohedral carbonates; C. Subsolidus phase relations; D. Activity-composition relations.

1 Introduction

The rhombohedral calcite-magnesite binary, (1-x)·$CaCO_3$-x·$MgCO_3$, is one of the most well studied solid solutions in mineralogy. The experimental study of Goldsmith and Heard (1961) identified the essential features of subsolidus phase relations: two asymmetric miscibility gaps separated by a narrow stability field for the dolomite-structure phase. Calorimetric studies by Navrotsky and Capobianco (1987), Chai et al. (1995), Chai and Navrotsky (1996) and Navrotsky et al. (1999) showed that the enthalpy of formation of ordered dolomite is negative, relative to a mechanical mixture of calcite and magnesite, but the formation enthalpy for a disordered solid solution of the same composition is positive. The magnitude of the enthalpy of disorder is unclear owing to different calorimetric results: 1.23 $\pm$ 0.32 (Navrotsky and Capobianco, 1987) for a heat-treated natural sample; and 16.5 $\pm$ 2.5 kJ/mol (Navrotsky et al., 1999) for a synthetic sample. Burton and Van de Walle (2003) published an extensive data set of formation energies for various ordered supercells, that were calculated with the Vienna ab initio simulation package, VASP (Kresse and Furthmüller, 1996). The VASP calculations also yield a negative formation energy for dolomite and first principles phase diagram calculations based on the VASP formation energies yield an enthalpy of mixing of $\sim$6 kJ/mol for the random solid solution at X=0.5. Various theoretical approaches including the Bragg-Willams model (Navrotsky, 1987; Davidson, 1994),

different approximations of the cluster variation method (Burton and Kikuchi, 1984; Burton, 1987) and Monte Carlo simulations (Burton and Van de Walle 2003; Purton et al., 2006) achieve qualitative or semi-quantitative agreement between predicted and experimentally determined phase relations. None of these studies, however, produced a mathematically simple activity-composition model consistent with experimental phase boundaries. Such a model is often requested for petrological and environmental studies which attempt phase equilibrium calculations in chemically complex systems. Here we derive activity-composition relations with static structure energy (SSE) calculations based on the well constrained set of empirical interatomic potentials of Rohl et al. (2003) and Austen et al. (2005). Calculations were performed in the following sequence:

- Testing the empirical interatomic potentials
- SSE calculations on a large set of randomly selected structures
- Fitting a cluster expansion, CE, to the SSE i.e. finding a mathematically simple equation that fits the excess SSE
- Ground state analysis, i.e. finding the structures with lowest SSE
- Monte Carlo simulations of temperature-dependent properties.
- Thermodynamic integration of the Monte Carlo results to calculate free energies of mixing
- Fit a polynomial to the Monte Carlo free energies and calculate activity-composition relations.

This sequence of calculations yields activity-composition relations, that agree almost quantitatively with the experimentally determined phase relations.

2 Empirical potentials

Rohl et al. (2003) and Austen et al. (2005) developed a set of interatomic potentials for carbonate minerals, which exhibit remarkable accuracy in reproducing the structures of calcite, dolomite, magnesite and aragonite; and available elastic stiffness data on calcite and magnesite. A good description of the structure and elasticity data does not, however, guarantee accurate predictions of energy differences between differently ordered supercells. To test the empirical-potential based GULP (Gale, 1997; Gale and Rohl,

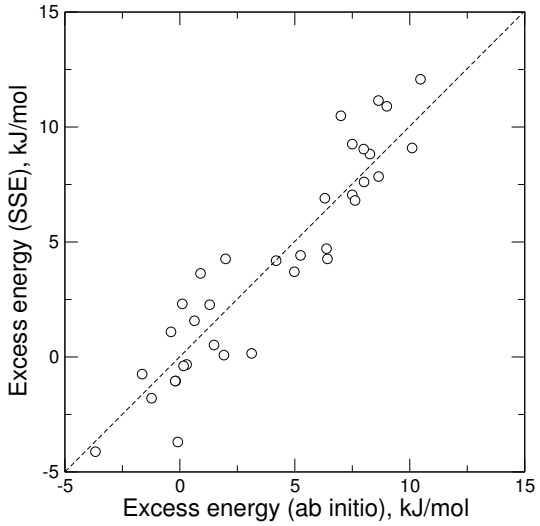

Figure 1: Correlation between the excess energies of a selected set of ordered structures calculated with parameterized force field (Austen et al., 2005) and VASP (Burton and Van de Walle, 2003) methods.

2003) SSEs, we compare them to VASP-SSE for the same set of ordered structures, that Burton and Van de Walle (2003) considered. In Fig. 1 we plot the GULP-SSE vs. VASP-SSE. The plot includes all structures described by Burton and Van de Walle (2003) except for the huntite, $Ca_3Mg(CO_3)_4$ structure, for which: SSE-GULP=28.72 kJ/mol; SSE-VASP=44.73 kJ/mol. This large difference in excess energy is related to the difference between CO_3-group orientations in huntite vs. that in calcite and magnesite. The good correlation between the GULP and VASP sets suggests that the Austen et al. (2005) potentials essentially reproduce the energetics of cation mixing/ordering.

3 Supercell SSE calculations

We use a 4x4x1 supercell of $R\bar{3}c$ calcite (a = 4.988Å, c = 17.061Å) that contains 96 exchangeable (Ca,Mg) atoms. We start in the ordered dolomite structure, in which Ca and Mg occupy alternate layers perpendicular to the c axis, and generate several structures, with compositions between calcite and magnesite, by replacing appropriate numbers of Ca or Mg atoms with Mg and Ca atoms, respectively. Cation distributions in structures with compositions $x = 0.125$, $x = 0.25$, $x = 0.375$, $x = 0.5$, $x = 0.625$, $x = 0.75$ and $x = 0.875$ were varied by randomly swapping selected atoms pairs. Swapping was repeated 100 times at each composition and fully relaxed static GULP-SSEs were calculated for each structure. Excess energies of these 700 structures are plotted in Fig. 2. This plot outlines only the general shape and magnitude of the enthalpy of mixing. Calculating enthalpy isotherms requires additional

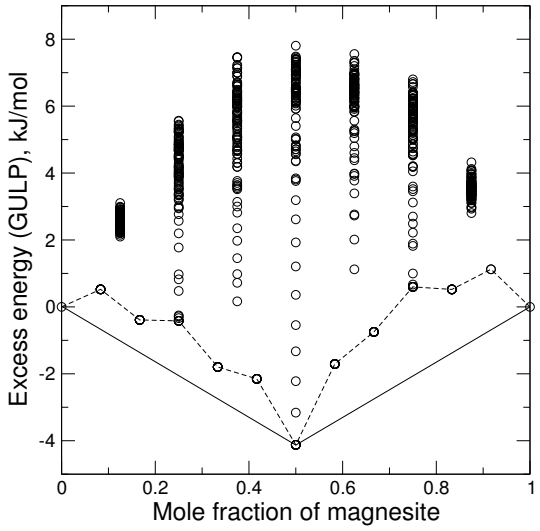

Figure 2: Excess static structure energies for 700 structures that were calculated with the interatomic potentials of (Austen et al., 2005). The dashed line connects minimum energy structures at each composition; calcite, dolomite and magnesite are the only predicted ground states (solid line).

effort.

4 The cluster expansion

Constructing isotherms requires Boltzmann averaging over many configurations at each composition in a sufficiently large supercell. Precise estimates of the average energies can be made with a Monte Carlo algorithm, but computational efficiency requires more rapid SSE calculations than GULP permits. Therefore, the cluster expansion (CE) method (Connolly and Williams, 1983; Sanchez et al., 1984) is used to speed up calculations. The CE is compact set of effective interactions, which in its simplest form (Dove, 1999; Becker et al., 2000; Vinograd, 2001) maps the excess energy, E_i, of structure-i onto a set of effective pair interactions, $J^{(n)}$; that are coupled to the frequencies of AB pairs, $f^{(n)}_{\mathrm{AB}}$ in structure-i:

$$E_i = 1/2 \sum_n f^{(n)}_{\mathrm{AB}} J^{(n)} + E_0, \tag{1}$$

n is the order of the near-neighbour pair, which increases with interneighbour separation, and E_0 is a configuration independent strain energy. In solid solutions with size mismatch E_0 represents the global strain that is caused by substituting smaller ions (Mg) into larger-ion-rich (Ca-rich) crystals, or larger ions (Ca) in smaller-ion-rich (Mg-rich) crystals. Ferreira et al. (1988) demonstrated that this strain energy is maximized at an intermediate composition, typically not $x = 0.5$, such that it varies

superquadradically with composition. We approximate this variation with a two-parameter polynomial:

$$E_0 = x_1 x_2 (x_1 A_{12} + x_2 A_{21}). \quad (2)$$

For each of the 700 structures we calculated frequencies of of AB-type (Mg-Ca) pairs at 12 distances ranging from 3.8 to 10.4 A. The frequencies and the energies form an overdetermined system of 700 equations, which were solved for $J^{(n)}$, A_{12} and A_{21} using a least-squares minimization.

Figure 3 is a plot of excess energies for the 700 structures that were calculated with the CE vs. those calculated with GULP. Each $J^{(n)}$ corresponds to the energy of the exchange reaction Ca-Ca + Mg-Mg = 2Ca-Mg at the n-th neighbor distance. Negative Js indicate an ordering tendency (Ca-Mg pairs favored) and positive values indicate a clustering tendency (Ca-Ca and Mg-Mg pairs favored). The best fit for E_0 was A_{12}=49.128 and A_{21}=36.542 kJ/mol. When only pair, or other even-order (pair=2-, 4-, 6-,... 2n-body) interactions are used, calculated phase diagrams have mirror symmetry about $x = 0.5$; thus, the E_0 term is the only source of phase diagram asymmetry in this model. The inequality $A_{12} \rangle A_{21}$ reflects the higher energy that is required to substitute larger Ca^{2+} ions into a Mg-rich crystal; relative to the smaller energy required to substitute a Mg^{2+} ion into a Ca-rich crystal. The Js are plotted in Fig. 4 as functions of interatomic separation. The remarkable feature of Fig. 4 is the large negative value of $J^{(4)}$. This result was interpreted as reflecting the high stiffness of the structure along the 4'th neighbor pair, caused by the presence of rigid CO_3 group between the exchangeable atoms (Vinograd, 2006a). Note however, that the Burton and Van de Walle (2003) CE predicts opposite character for $J^{(4)}$, such that it favors Ca-Ca and Mg-Mg 4'th neighbor pairs. The essential differences between the CE derived here and the CE in Burton and Van de Walle (2003) are that the latter: 1) includes some 3-body effective interactions, which determine phase diagram asymmetry; 2) does not include an E_0 term; 3) uses a cross validation score statistical test to chose which Js to include in the CE and which VASP structure energies to use for fitting the CE. The cross validation score test has two significant advantages relative to least squares: 1) the CE is optimized for *accuracy of prediction* rather than minimization of residuals; 2) the number of effective interactions in the CE optimized rather than arbitrarily truncated.

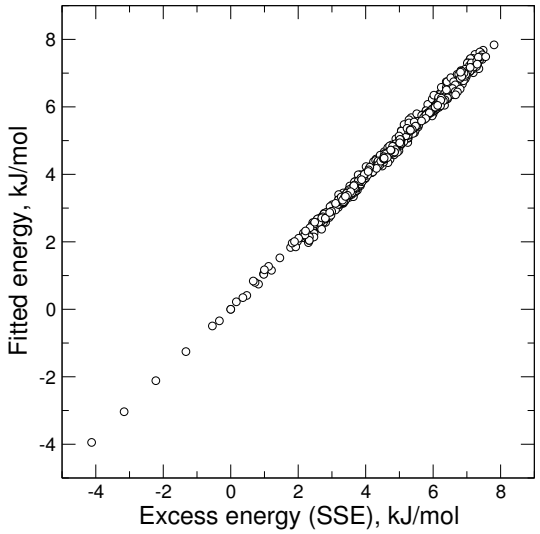

Figure 3: Correlations between the energies of 700 structures calculated with GULP and those calculated with the cluster expansion).

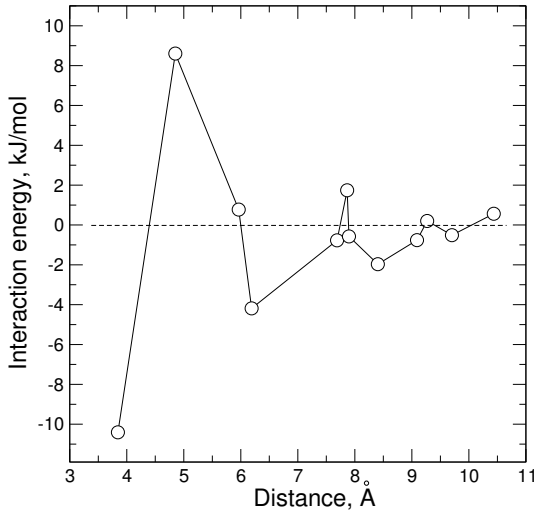

Figure 4: The cluster expansion of pair-wise effective interactions for the calcite-magnesite system as functions of interatomic separation.

Table 1: Pair-wise effective interactions and their type: 1-interlayer, 2-intralayer.

n	Distance, Å	Type	J_n, kJ/mol
1	3.844	1	-10.200
2	4.852	2	8.563
3	5.964	2	0.931
4	6.190	1	-3.863
5	7.688	2	-0.780
6	7.865	1	1.991
7	7.897	1	-0.982
8	8.403	2	-1.655
9	9.091	2	-0.826
10	9.269	1	-0.111
11	9.703	2	-0.305
12	10.437	1	0.610

5 Ground state analysis

Figure 3 shows that Equation 1 provides a good fit to the 700 randomly generated configurations. This does not, however, ensure that the CE will correctly predict ground states. Low-energy structures in the 4x4x1 supercell were predicted with Monte Carlo annealing simulations, with the feedback algorithm of Vinograd et al. (2006b): 1) the temperature is set at a high value, then slowly decreased until exchangeable atoms freeze into the state of lowest energy; 2) the GULP-SSE for this structure is calculated, and often this energy differs significantly from the CE-calculated value; 3) the CE is updated and steps 1) and 2) are repeated. The quality of the CE improves automatically. When the energy difference between CE- and GULP-calculated energies is large, the correlation coefficient goes down significantly and the Js and A_{ij} change to improve the fit. The CE-predicted minima, (including ground states at $x = 0,\ 1/2,\ and\ 1.0$) are plotted together with the energies of randomly selected structures in Fig. 2. Consistent with Burton and Van de Walle (2003), we find that dolomite + calcite and dolomite + magnesite are the only stable ground state assemblages. The final CE pair interactions are listed in Table 1. Final values for the E_0 parameters are $A_{12} = 46.447$ kJ/mol and $A_{21} = 34.151$ kJ/mol; similar to those calculated from the set of randomly selected structures, A_{12}=49.128 kJ/mol and A_{21}=36.542 kJ/mol.

6 Monte Carlo simulations

Rapid convergence of the CE as a function of interatomic separation (Fig. 4) suggests that Equation 1 is applicable for calculations of excess energies in a much larger supercell. Sufficient supercell size for thermodynamically meaningful results can be estimated by performing Monte Carlo simulations in supercells of increasing size. The thermodynamic limit is achieved when the predicted properties such as temperatures of order/disorder transitions does not change with the further increase in the size of the supercell. In this study we have used the 12x12x3 supercell of calcite containing 2592 exchangeable atoms. Additional calculations using 16x16x4 supercell (6144 atoms) have shown that the simulated temperature of the order/disorder transition at dolomite composition (T=1345$\pm$ 25 K) does not differ within the error limits from the result obtained with the 12x12x3 supercell (Fig. 5). The smaller supercell was used then for the calculations of the thermodynamic properties. At each step of the Monte Carlo run we create a new configuration by swapping a randomly chosen pairs of cations. The acceptance probability, ξ, for a candidate configuration depends on temperature and the energy difference, ΔE, between the two configurations

$$\begin{aligned} \xi = 1,\ \Delta E < 0 \\ \xi = exp(-\Delta E/(kT)),\ \Delta E > 0 \end{aligned} \tag{3}$$

This acceptance rule converges the *set* of configurations to the Boltzmann distribution (Metropolis et al. 1953). Simulations were performed on a grid of 48 compositions between calcite and dolomite and 15 temperatures between 623 and 2023 K. Six billion Monte Carlo steps were used to achieve equilibrium and another six billion steps were used to calculate averages. These simulations were performed with a constant $E_0 = 0$ term to suppress phase separation; a procedure that necessarily yields a phase diagram with mirror symmetry about $x = 0.5$. Composition-dependent E_0 values and average enthalpies were subsequently combined to calculate enthalpy of mixing isotherms (Fig. 6).

7 Thermodynamic integration

Myers et al. (1998) and Dove (2001) demonstrated that the configurational free energy can be calculated from Monte Carlo averaged excess energies via $\lambda-$integration:

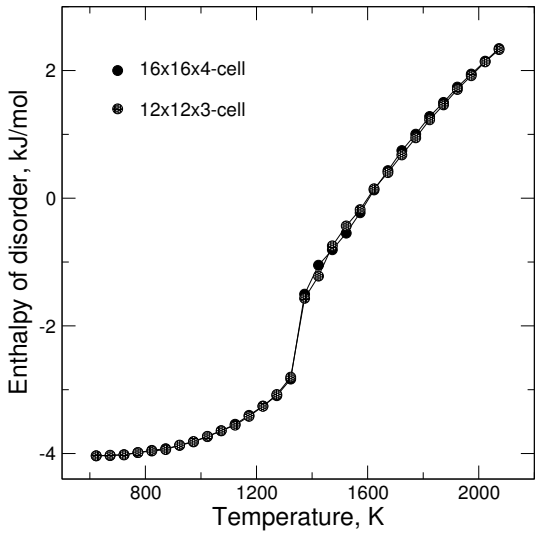

Figure 5: Enthalpy of disorder at the dolomite composition calculated with the Monte Carlo method.

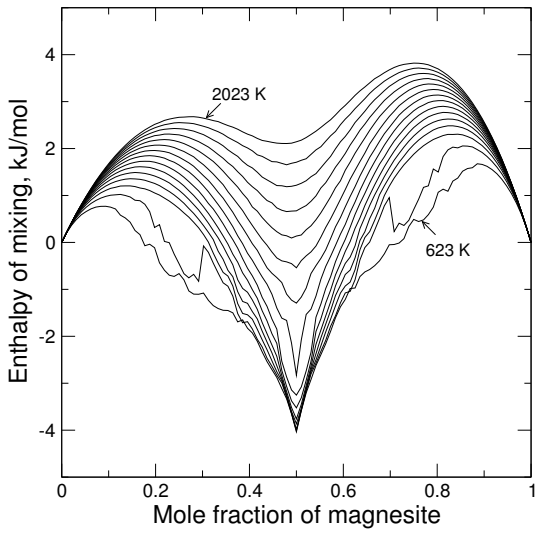

Figure 6: Enthalpy of mixing isotherms calculated with the Monte Carlo method.

$$F = F_0 + \int_0^{\lambda} E_\lambda d\lambda. \tag{4}$$

F_0 is the free energy of mixing of the solid solution with zero ordering energy, which can be calculated theoretically:

$$F_0 = RT(x_{\mathbf{Mg}} \ln(x_{\mathbf{Mg}}) + x_{\mathbf{Ca}} \ln(x_{\mathbf{Ca}})). \tag{5}$$

E_λ is the average energy of the system in a state with a non-equilibrium intermediate degree of order which is defined by λ, $0 < \lambda < 1$. The integral describes the change in free energy as the degree of order changes from zero to its equilibrium value. An intermediate degree of order is simulated by scaling the Js according to the equation J_n^{λ}=λJ_n. In our simulations, λ was gradually increased from 0 to 1 with a step size of 0.04.

Computational times required for these free energies of mixing, which include temperature dependent configurational entropies, were 26 times longer than those for enthalpies. Configurational entropy isotherms were calculated with

$$S = (F - E)/T \tag{6}$$

and are plotted in Figure 7. The remarkable features of this plot are the minima at $x = 0.5$, $x = 0.25$ and $x = 0.75$. The sharp minimum at $x = 0.5$ is caused by dolomite-type ordering, and the two broad minima at $x = 0.25$ and $x = 0.75$ correspond to dolomite-related structures that have different stacking sequences for Ca- and Mg-rich layers. The Monte Carlo simulated low-temperature cation distribution at $x = 0.25$ (Fig. 8) is the ϵ-dolomite structure, which is a layer structure with layer-sequence Mg-Ca-Ca-Ca-...perpendicular to c_{hex}. The Mg-Ca-Ca-... sequence (δ-dolomite) is also observed locally, but because the supercell with 18 layers in the z direction is incommensurate with the four-layer sequence, its' low-energy structure is not explicitly calculated. Metastable formation of ϵ-dolomite is consistent with the first principles calculations of Burton and Van de Walle (2003), which suggested that ϵ-dolomite has the lowest formation-energy at $x = 1/4$ and $x = 3/4$.

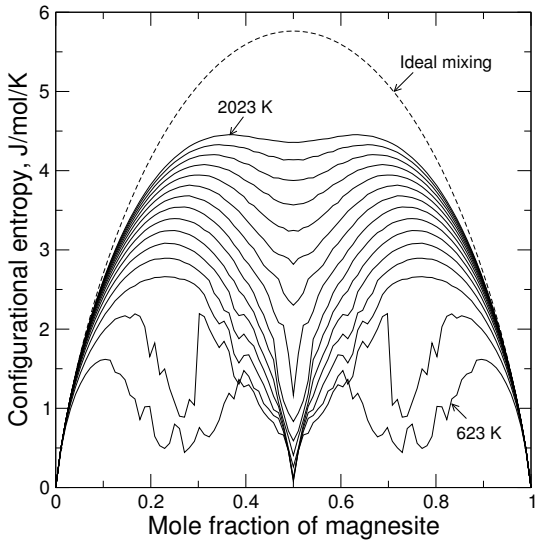

Figure 7: Configurational entropy isotherms that were calculated by thermodynamic integration.

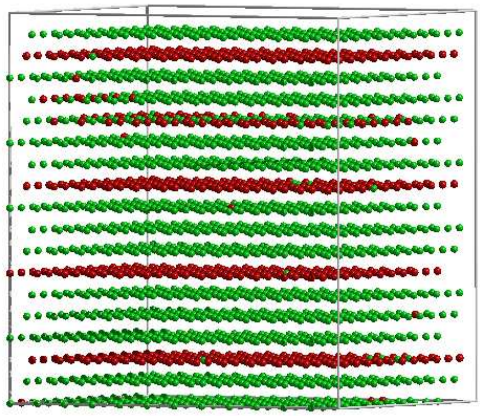

Figure 8: Monte Carlo simulated cation distribution (Ca-red, Mg-green) at x=0.25, T=623 K.

8 The phase diagram

Free energies of mixing are plotted in Fig. 9. They were converted to a phase diagram by: comparing the free energy at each composition x_i along an isotherm to the free energy of a mechanical mixture $x_j + x_k$. If there is a pair of compositions $x_j + x_k$, that has lower free energy, the solution with composition x_i is unstable or metastable (white in Fig. 10) The two miscibility gaps separated by the dolomite field are easily outlined. The calculated diagram is compared to experimental data from Goldsmith (1983), and agreement is nearly quantitative. The difference is that in the calculated diagram the miscibility gap on the Ca-rich side is slightly shifted to more Ca-rich compositions.

9 Activity-composition relations

Redlich-Kister polynomials (Redlich and Kister, 1948) are convenient for describing excess free energies of mixing, but these equations fail in systems with strong ordering at intermediate compositions. The rapid decrease in free energy from dolomite-ordering at x =0.5 can be parameterized with negatively shaped gaussians. The combination of Redlich-Kister polynomials and gaussians is very effective for fitting free energies of mixing in systems with intense ordering at intermediate compositions (e.g. Vinograd, 2002; Vinograd and Sluiter, 2006). The total excess free energy of mixing can be described with the equation

$$G_{excess} = x_1 x_2 \sum_{i=1}^{n} A_i (x_1 - x_2)^{(i-1)} + x_1 x_2 \sum_{j=1}^{m} B_J \exp(C_j (x_1 - x_j)^2) \tag{7}$$

where A_i, B_i and C_i are further expanded as functions of temperature $A_i = A_i^h - TA_i^s$, $B_i = B_i^h - TB_i^s$, $C_i = C_i^h - TC_i^s$; x_1 and x_2 are the mole fractions of end-members; and $x_j$is the mole fraction, of ordered compound j. Figure 9 illustrates the accuracy of Eqn. 7-fit to Monte Carlo simulated free energies of mixing. The A_i, B_i and C_i coefficients are listed in Tables 2 and 3. Figure 11 is a plot of activity-composition relations, which were derived from fitted free energies of mixing.

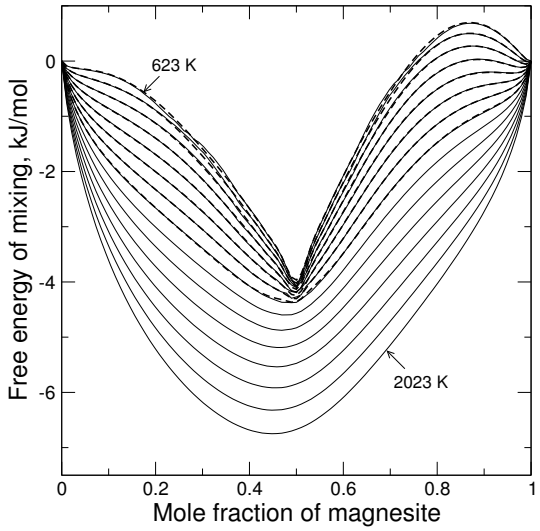

Figure 9: Free energy of mixing isotherms calculated by thermodynamic integration (solid lines) and fit to Equation 7 (dashed lines). The fit applies only to the temperature range 623-1323 K.

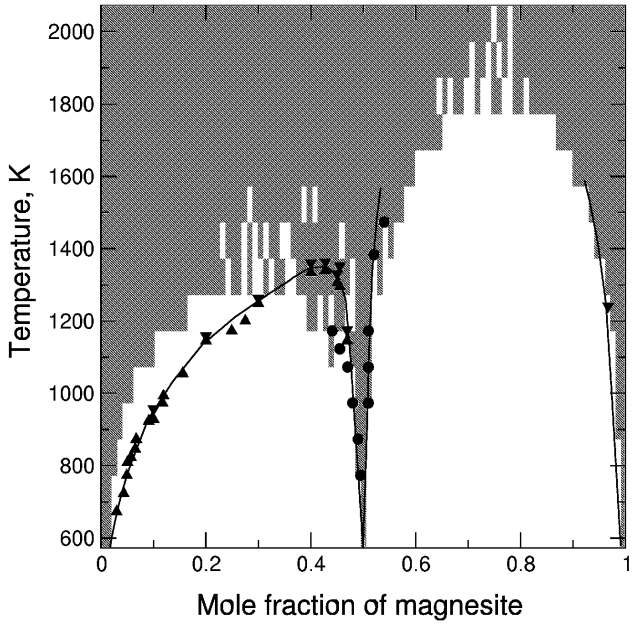

Figure 10: The calcite-magnesite phase diagram. Gray and white areas indicate stable and unstable (or metastable) states, respectively; predicted by Monte Carlo simulations. Symbols and solid lines are experimental data from Goldsmith (1983).

Table 2: Coefficients of the Redlich-Kister polynomial (A_i^h in kJ/mol, A_i^s in kJ/K/mol)

i	A_i^h	$A_i^s * 10^3$
1	11.8948	-3.2801
2	6.0778	-0.0866
3	5.6420	-8.5177
4	0.5705	0.5624
5	10.5240	12.4392
6	-0.6759	-0.6519

Table 3: Coefficients of the gaussians (B_i^h and C_i^h in kJ/mol, B_i^s and C_i^s in kJ/K/mol)

j	x	B_j^h	$B_j^s * 10^3$	C_j^h	C_j^s
1	0.50	-16.7374	-10.6106	10.1136	0.0388
2	0.50	-5.9028	-4.3690	8.5369	0.2051
3	0.5	-3.7182	-2.5465	-447.3994	1.2768

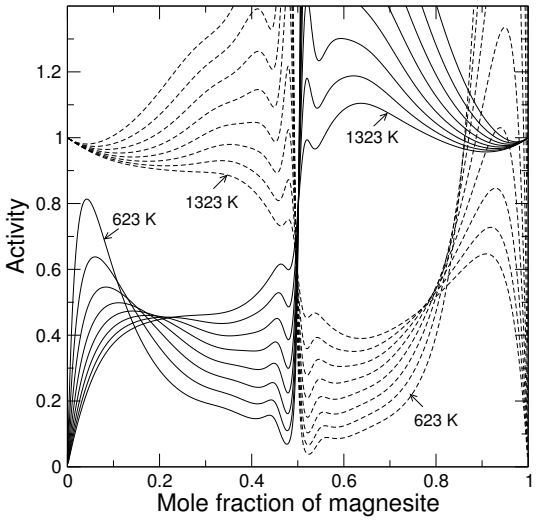

Figure 11: Fitted activities of calcite and magnesite (solid and dashed lines, respectively) in the interval 623-1323 K.

10 Discussion and Conclusions

Realistic activity-composition relations for carbonates were calculated with well-constrained empirical interatomic potentials. Good agreement between predicted and experimentally determined phase relations indicates that the simulations reproduce the main thermodynamic effects of mixing and cation order/disorder in the rhombohedral carbonates. The main difference between experiment and calculation is that the Ca-rich calcite + dolomite field is slightly shifted to more Ca-rich compositions. This might be the result of performing the simulations in the static limit. Burton and van de Walle (2006) demonstrated that including excess vibrational entropy in a first principles phase diagram calculation for the system NaCl-KCl leads to a dramatic improvement in the calculated consolute temperature. Also, Vinograd and Sluiter (2006) have shown that excess vibrational entropy plays a significant role in the subsolidus phase relations of pyrope-grossular, $Mg_3Al_2Si_3O_{12}$ - $Ca_3Al_2Si_3O_{12}$, garnets. Both the experimental data (Haselton and Westrum, 1980; Dachs and Geiger, 2006) and the calculations (Vinograd and Sluiter, 2006) show that the excess entropy in Ca-Mg-garnets achieves about 1-1.5 J/K per mole of exchangeable atoms at intermediate compositions. Vinograd and Sluiter (2006) demonstrated that the positive excess entropy in the pyrope-grossular system appears as a consequence of the size-mismatch between end-members. Their results suggested also that the maximum of the excess effect is shifted in the direction of the end-member with the largest volume. If the same trend holds for carbonates, the excess entropy would make Ca-rich compositions more stable, and this would improve agreement between calculations and experiment. This assumption should be tested in future simulation studies.

The predicted excess enthalpy for ordered dolomite, -4.0 kJ/mol, is in good agreement with the experimental value, -5.74 $\pm$ 0.25 kJ/mol [Navrotsky and Capobianco (1987)] and with the ab initio VASP result, -3.66 kJ/mol, [Burton and Van de Walle (2003)]. The predicted equilibrium excess enthalpy of dolomite, -0.5 kJ/mol at 1523 K 5, is in reasonable agreement with the value of 1.23 $\pm$ 0.32 kJ/mol measured by Navrotsky and Capobianco (1987) for a sample of Eugui dolomite that was heat-treated at 1523K. The value of 16.5 $\pm$ 2.5 kJ/mol measured by Navrotsky et al. (1999) for a synthetic disordered dolomite cannot be explained by the present model. According to our simulations (Fig. 2), a random Ca/Mg configuration contributes only 6-8 kJ/mol to the excess enthalpy of dolomite. The present model also contradicts calorimetric measurements of Chai et al. (1995), which suggested that the enthalpies of formation of diagenetic Ca-rich dolomites are significantly higher than those of isochemical

calcite + magnesite mechanical mixtures. Note that our model only includes the effects of the cation order/disorder, and ignores orientational order-disorder of the CO_3 groups. The CO_3-group orientational order-disorder ($R\bar{3}c$/ $R\bar{3}m$) transition in calcite occurs at about 1260 K (Dove and Powell, 1989; Dove et al. 2005). It is possible that some CO_3-group disordering could be quenched during the heat treatments of natural dolomite samples. This effect might explain the difference of 1.72 kJ/mol between the excess energy of the heat-treated dolomite measured by Navrotsky and Capobianco (1987) and our value of -0.5 kJ/mol at 1523 K. The very large value of the excess energy of 16.5 $\pm$ 2.5 kJ/mol measured by Navrotsky et al. (1999) for a synthetic dolomite might be caused by orientational disorder. The low temperature of the synthesis (70 °C) might not be sufficient for CO_3 groups to reorder themselves into to the lowest energy configuration. The same argument might apply to the high excess enthalpies of diagenetic Ca-rich dolomites measured by Chai et al. (1995). VASP calculations of Burton and Van de Walle (2003) have shown the very high energy of formation for huntite-structure $Ca_3Mg(CO_3)_4$ (a structure, in which CO_3-group orientation differs from that of calcite and dolomite). This structure was derived from the naturally occurring $Mg_3Ca(CO_3)_4$ huntite (Dollase and Reeder, 1986) by substituting Ca for Mg and Mg for Ca. The very high formation energy of this structure (44.73 kJ/mol (VASP), 28.72 kJ/mol (GULP)) suggests that even a small concentration of huntite-like domains could significantly increase enthalpies of formation in Ca-rich dolomites. Transmission electron microscopy studies of Ca-rich dolomites in pre-Holocene rocks often reveal modulation with lamellar spacing of 100-200 Å (Wenk et al. 1983). Crystal structure refinements of two such samples within the $R\bar{3}$ space group of dolomite have shown poor fits and indicated that one of the components of the modulated structure should have mixed occupancy in cation layers (Reeder, 2000). Huntite, $Ca_3Mg(CO_3)_4$, having mixed (ordered) arrangement of Ca and Mg in dolomite-like cation layers satisfies this criterion. An increase in the fraction of huntite-like domains within the modulated structure could explain the correlation of the excess enthalpies of Ca-rich dolomites with mole fraction of calcite (Chai et al., 1995). This hypothesis should be tested in future simulation studies, and by electron microscopy studies of natural samples. Success of the present model in reproducing the phase diagram without accounting for phases with CO_3-group orientational disorder suggests, however, that the miss-orientation of the CO_3-groups plays a minor role in determining equilibrium subsolidus phase relations. The very high formation energies of these structural defects is consistent with the observation of Reeder and Nakajima (1982) that thermal disorder of dolomite produces twin domains boundaries (TDB) rather than anti-phase boundaries (APB). The difference is that

an APB implies misaligned CO_3-groups as well as misaligned cation layers, whereas the TDB only has a cation mismatch, without CO_3-group orientational mismatch.

Acknowledgments

The present investigation was supported by Deutsche Forschungsgemeinschaft (Project Wi-1232/14-2). JDG would like to thank the Government of Western Australia for funding under the Premiers's Research Fellowship program.

References

Austen K., Wright K., Slater B. and Gale J.D. (2005) The interaction of dolomite surfaces with metal impurities: a computer simulation study. *Physical Chemistry Chemical Physics* **7**, 4150-4156.

Becker U., Fernandez-Gonzalez A., Prieto M., Harrison R. and Putnis A. (2000) Direct calculation of thermodynamic properties of the barite/celectite solid solution from molecular principles. *Physics and Chemistry of Minerals* **27**, 291-300.

Burton B.P. (1987) Theoretical analysis of cation ordering in binary rhombohedral carbonate systems. *American Mineralogist* **72**, 329-336.

Burton B.P. and Kikuchi R. (1984) Thermodynamic analysis of the system $CaCO_3$ -$MgCO_3$in the tetrahedron approximation of the cluster variation method. *American Mineralogist* **69**, 165-175.

Burton B.P. and Van de Walle A. (2003) First Principles Based Calculations of the $CaCO_3$ -$MgCO_3$Subsolidus Phase Diagrams. *Physics and Chemistry of Minerals* **30**, 88-97.

Burton B.P. and van de Walle A. (2006) First principles phase diagram calculations: the role of excess vibrational entropy. *Chemical Geology* **225**, 222-229.

Burton B.P., Dupin N., Fries S.G., Grimvall G., Fernandez Guillermet A., Miodownik P., Oates W.A. and Vinograd V. (2001) Using 'Ab Initio' Calculations in the Calphad Environment. *Zeitschrift für Metallkunde* 92 **6**, 514-525.

Chai L. and Navrotsky A. (1996) Synthesis, characterization, and energetics of solid solution along the $CaMg(CO_3)_2$ -$CaFe(CO_3)_2$ join and implication for the stability of ordered $CaFe(CO_3)_2$. *American Mineralogist* **81**, 1141-1147.

Chai L., Navrotsky A. and Reeder R.J. (1995) Energetics of calcium-rich dolomite. *Geochimica et Cosmochimica Acta* **59**, 939-944.

Connolly J.W.D. and Williams A.R. (1983) Density-functional theory applied to phase transformations in transition-metall alloys. *Physical Review* **B27**, 5169-5172.

Dachs E. and Geiger Ch.A. (2006) Heat capacities and entropies of mixing of pyrope-grossular ($Mg_3Al_2Si_3O_{12}$ -$Ca_3Al_2Si_3O_{12}$) garnet solid solutions: A low temperature calorimetric and a thermodynamic investigation. *American Mineralogist* (in press).

Davidson P.M. (1994) Ternary iron, magnesium, calcium carbonates: A thermodynamic model for dolomite as an ordered derivative of calcite-structure solutions. *American Mineralogist* **79**, 332-339.

Dollase W.A., Reeder R.J. (1986) Crystal structure refinement of huntite, $Ca_3Mg(CO_3)_4$, with X-ray power data. *American Mineralogist* **71**, 163-166.

Dove M.T. (1999) Order/disorder phenomena in minerals: ordering phase transitions and solid solutions. In *Microscopic properties and processes in minerals. NATO ASI Ser. C* **543** (eds. K. Wright and R. Catlow) Dordrecht, Kluwer, Dordrecht, pp 451-475.

Dove M.T. (2001) Computer simulations of solid solutions. In *Solid Solutions in Silicate and Oxide Systems of Geological Importance. EMU Notes in Mineralogy* **3** (ed. Ch. Geiger) Eötvös University Press, Budapest, pp. 245-249.

Dove M.T. and Powell B.M. (1989) Neutron powder diffraction study of the tricritical orientational order-disorder phase transition in calcite at 1260 K. *Physics and Chemistry of Minerals* **16**, 503-507.

Dove M.T., Swainson I.P., Powell B.M. and Tennant D.C. (2005) Neutron powder diffraction study of the orientational order-disorder phase transition in calcite, $CaCO_3$. *Physics and Chemistry of Minerals* **32**, 493-503.

Ferreira L.G., Mbaye A.A. and Zunger, A. (1988) Chemical and elastic effects on isostructural phase diagrams: The e-G approach. *Physical Review B* **37**, 10547-10570.

Haselton, Jr.,H.T. and Westrum, Jr.,E.F. (1980) Low-temperature heat capacities of synthetic pyrope, grossular, and pyrope$_{60}$grossular$_{40}$. *Geochimica et Cosmochimica Acta* **44**, 701-709.

Goldsmith (1983) Phase relations of rhombohedral carbonates. In Reeder R.J. (ed) *Reviews in Mineralogy* **11**, 49-76.

Gale, J.D. (1997) GULP - a computer program for the symmetry adapted simulation of solids. *Journal of Chemical Society: Faraday Transactions* **93**, 629-637.

Gale J.D. and Rohl A.L. (2003) The General Utility Lattice Program (GULP). *Molecular Simulations* **29**, 291-341.

Goldsmith, J.R., and Heard, H.C. (1961) Subsolidus phase relations in the system $CaCO_3$ -$MgCO_3$. *Journal of Geology* **80**, 611-626

Kresse, G. and Hafner, J., Ab initio molecular dynamics for liquid metals Phys. Rev. **B47**: 558-561 (1993); Kresse, G. Thesis, Technische Universität Wien 1993; Phys. Rev. **B49**: 14 251 (1994). Kresse, G. and Furthmüller, J. (1996) Efficiency of ab-initio total energy calculations for metals and semiconductors using a plane-wave basis set Comput. Mat. Sci. **6**: 15-50; Efficient iterative schemes for ab initio total-energy calculations using a plane-wave basis set Phys. Rev. **B54**: 11169 (1996); cf. http://tph.tuwien.ac.at/ vasp/guide/vasp.html.

Metropolis N.I., Rosenbluth A.W., Rosenbluth M.N., Teller A.N. and Teller, E. (1953) Equation of state calculations by fast computing machines. *Journal of Chemical Physics* **21**, 1087-1092.

Myers E.R., Heine V. and Dove M.T. (1998) Some consequences of Al/Al avoidance in the ordering of Al/Si tetrahedral framework structures. *Physics and Chemistry of Minerals* **25**, 457-464.

Navrotsky A. (1987) Models of crystalline solutions. In *Rewiews in Mineralogy* **17** (ed. R.J. Reeder), Mineralogical Society of America, Washington DC, pp. 35-69.

Navrotsky A. and Capobianco C. (1987) Enthalpies of Formation of Dolomite and of Magnesian Calcites. *American Mineralogist* **72**, 782-787.

Navrotsky A., Dooley D., Reeder R. and Brady P. (1999) Calorimetric Studies of the Energetics of Order-Disorder in the System $Mg_xFe_{1-x}Ca(CO_3)_2$. *American Mineralogist* **84**, 1622-1626.

Purton J.A., Allan N.L., Lavrentiev M.Yu., Todorov I.T. and Freeman C.L. (2006) Computer simulation of mineral solid solutions. *Chemical Geology* **225**, 176-188.

Reeder R.J. (2000) Constraints on cation order in calcium-rich sedimentary dolomite. *Aquatic Geochemistry* **6**, 213-226.

Reeder R.J., Nakajima, Y. (1982) The nature of ordering and ordering defects in dolomite. *Physics and Chemistry of Minerals* **8**, 29-35.

Redlich O. and Kister A.T. (1948) Thermodynamics of non-electrolyte solutions, x-y-t relations in a binary system. *Industrial and Engineering Chemistry* **40**, 341-345.

Rohl A.L., Wright K. and Gale J.D. (2003) Evidence from surface phonons for the (2x1) reconstruction of the (10-14) surface of calcite from computer simulation. *American Mineralogist* **88**, 921.

Sanchez J.M., Ducastelle F. and Gratias D. (1984) Generalized cluster description of multicomponent systems. Physica **128A**, 334-350.

Vinograd V.L. (2001) Configurational entropy of binary silicate solid solutions. In *Solid Solutions in Silicate and Oxide Systems of Geological Importance. EMU Notes in Mineralogy* **3** (ed. Ch. Geiger) Eötvös University Press, Budapest, pp. 303-346.

Vinograd V.L. (2002) Thermodynamics of mixing and ordering in the diopside-jadeite system: II. A polynomial fit to the CVM results. *Mineralogical Magazine* **66**, 537-545.

Vinograd V.L., Sluiter M.H.F. (2006) Thermodynamics of mixing in pyrope - grossular, $Mg_3Al_2Si_3O_{12}$ - $Ca_3Al_2Si_3O_{12}$, solid solution from lattice dynamics calculations and MonteCarlo simulations. *American Mineralogist* (in press)

Vinograd V.L., Sluiter M.H.F., Winkler B., Putnis A., Hålenius U., Gale J.D. and Becker U. (2004) Thermodynamics of mixing and ordering in the pyrope-grossular solid solution. *Mineralogical Magazine* **68**, 101-121.

Vinograd V.L., Winkler B., Putnis A., Gale J.D. and Sluiter M.H.F (2006a) Static lattice energy calculations of mixing and ordering enthalpy in binary carbonate solid solutions. *Chemical Geology* **225**, 304-313.

Vinograd V.L., Winkler B., Putnis A., Kroll H., Milman V., Gale, J.D. and Fabrichnaya, O.B. (2006b) Thermodynamics of pyrope - majorite, $Mg_3Al_2Si_3O_{12}$ -$Mg_4Si_4O_{12}$, solid solution from atomistic model calculations. *Molecular Simulations* (in press)

Wenk H-R., Barber D.J., Reeder R.J. (1983) Microstructures in carbonates. In Reeder R.J. (ed) *Reviews in Mineralogy* **11**, 301-367.

Wenk H-R., Meisheng Hu, Lindsley T. and Morris, Jr., J.W. (1991) Superstructures in ankerite and calcite. *Physics and Chemistry of Minerals* **17**, 527-539.